

State Estimation of Satellites using Ground Radar

Mitchell Krouss

April 28th 2024

1 Introduction/Background

1.1 Background Information

The goal of my research is to help develop data processing techniques for Space Situational Awareness (SSA). SSA, is the “knowledge, characterization, and practice of tracking space objects and their operational environments” defined by the Aerospace Corporation 4. SSA is important for predicting conjunctions between objects and helps enable collision avoidance maneuvers. The U.S. government is responsible for keeping an accurate map of all space traffic which can be distributed commercially 4. The 18th Space Control Squadron (18 SPCS) works with agencies from the UK, Canada, and Australia to form the Combined Space Operations Center (CSpOC). The CSpOC has both radar and optical sensors that measure Resident Space Objects (RSOs) and form the Space Sensor Network (SSN) 1. The CSpOC keeps a catalog of all RSOs they track. Data from these sensors are collected and processed to maintain an accurate map of RSOs.

1.2 Data

On January 24, 2021, a SpaceX Falcon 9 vehicle launched 143 small satellites into a Low Earth Orbit (LEO), with an altitude around 500 km 7. Figure 1 shows the number of RSOs which enter the catalog kept by CSpOC since the Transport-1 launch 1. It takes over 100 days to estimate the number of objects and their orbits. Out of the 143 satellites deployed, 139 are currently being tracked by CSpOC.

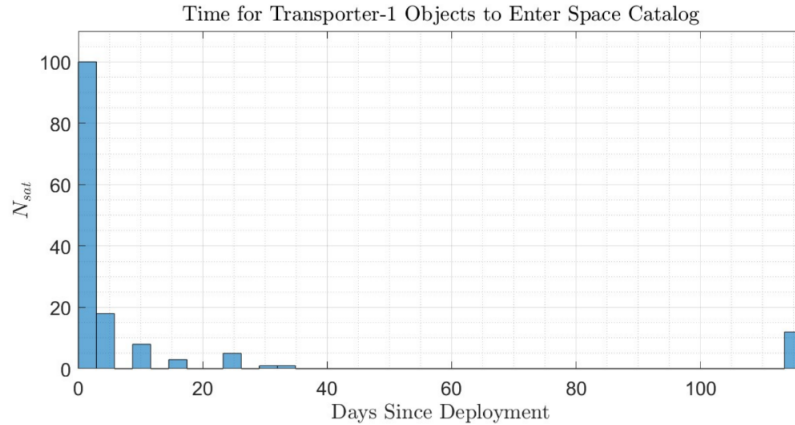


Figure 1: The number of RSOs which were entered in the CSpOC catalog since the Transport-1 deployment. 1

The US Air Force (USAF) provided a data set which contains radar measurements of the Transport-1 deployment. These radars make up part of the SSN. Figure 2 shows the locations of the different radars. Some of the radars are close to each other while others are further away. This can lead to long periods where there are no measurements for an RSO.

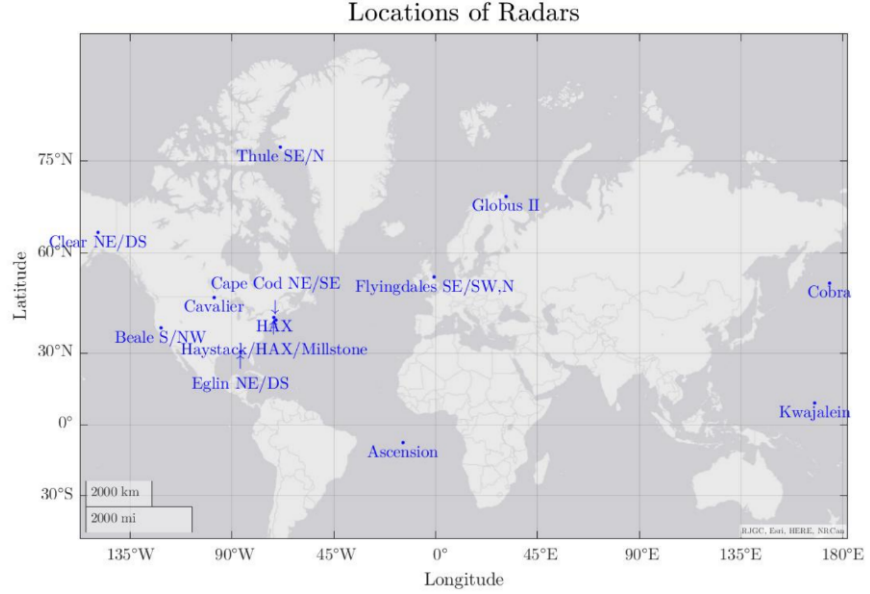


Figure 2: The location of the radars which make up the SSN. 1

Figure 3 shows a picture of the radar at Fylingdales. These radars can be hundreds of feet off the ground and have phased arrays which point in different directions. When a satellite passes out of the field of regard for one phased array, it will pass into the field of regard for the next phased array. This is useful data for comparing the orbits estimated in the individual phased arrays.



Figure 3: Radar at Fylingdales. https://en.wikipedia.org/wiki/RAF_Fylingdales

Each radar measurement provides azimuth and elevation angles, range, and

range rate. This data along with the radar station locations enable us to estimate the position and velocity of a satellite.

1.3 Previous Work

Davies and Doctor Axelrad implemented a Generalized Labeled Multi-Bernoulli (GLMB) Filter for Resident Space Object (RSO) tracking 1. This algorithm uses finite set statistics and Extended Kalman Filters (EKF) for data association and state estimation. Data association correlates satellite measurements with existing tracks. State estimation provides the ECI position and velocity for each track. Davies and Doctor Axelrad looked at cardinality as a metric to measure the performance of the filter. Cardinality is the number of satellites the algorithm estimates. Davies and Axelrad saw the algorithm correctly estimate cardinality on simulated data. However, when the algorithm was tested with real data, it overestimated the number of satellites which existed. Figure 4 compares the number of satellites estimated from the CSPOC catalog and the GLMB algorithm.

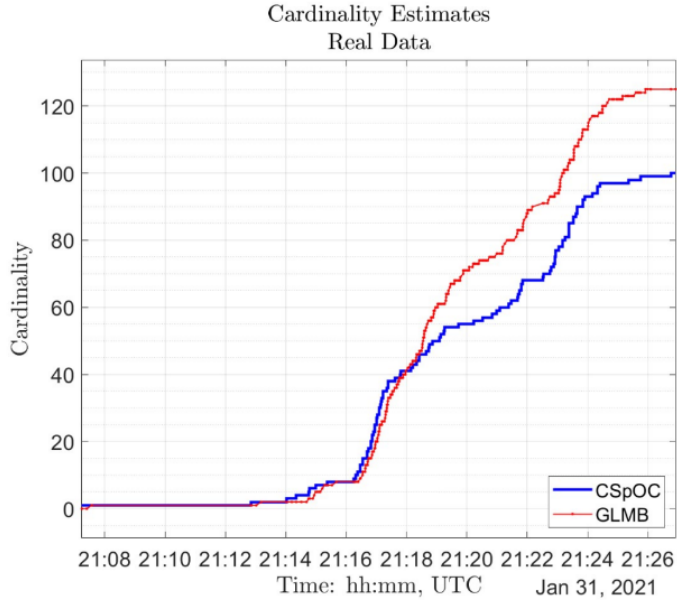


Figure 4: Cardinality estimates of the CSPOC catalog and the GLMB algorithm over time. 1

At the end of the 18 minutes, the GLMB algorithm estimated many more satellites compared to the CSPOC catalog.

1.4 Goal

Davies and Doctor Axelrad noticed that after long periods of propagation, with no measurements, the algorithm had difficulty associating new measurements to existing tracks. One potential reason why this could occur is the algorithm has poor state estimation at the end of a radar pass. When that state is propagated to the next radar pass, the errors grow, and the measurements look like different objects compared to the existing tracks. For this reason, I chose to focus on the state estimation part of the problem. I used an Extended Kalman Filter (EKF) for the state estimation algorithm.

2 Methods/Results

2.1 Extended Kalman Filter

A Kalman filter is a state estimation tool. The states are Earth Centered Inertial (ECI) position and velocity for each satellite. Kalman filters optimally update the state according to the measurement noise and the process noise of our system so that the mean squared errors of the states are minimized. The measurement noise is driven by the precision of the sensor. The expected distribution of the measurement errors is normal with mean zero and $\sigma_{range} = 10$ meters, $\sigma_{range_rate} = 1$ meter/second, $\sigma_{az} = 5e - 3$ degrees, and $\sigma_{el} = 5e - 3$ degrees. EKFs are preferred for nonlinear state estimation. Both the measurement model and dynamics model are nonlinear. The measurement model takes the azimuth, elevation, range, range rate to ECI position and velocity. The measurement model creates a Cartesian position vector in the SEZ frame with the azimuth, elevation, and the range. The vector is rotated into the Earth Centered Earth Fixed (ECEF) frame using a Directional Cosine Matrix (DCM) computed from the sensor's latitude, longitude, and altitude. The ECEF position is then rotated to the ECI coordinate frame. The dynamics model propagates our orbit over time. Numerical integration methods with and a two-body propagation and J2 perturbation were used for our dynamics model. The J2 perturbations account for the earth being an ellipsoid and not a sphere. The covariance propagation and update rely on Jacobians from the measurement and dynamics models.

The steps of the EKF are as follows. The EKF is initialized with a starting state, \hat{x}_0^+ , and a starting covariance, \hat{P}_0^+ . The subscript denotes the time step, and the superscript denotes if the quantity is before or after the measurement update. A $-$ is before a measurement update and a $+$ is after a measurement update. For each time step, a propagation is computed, at $k + 1$.

$$\hat{x}_{k+1}^- = f(\hat{x}_k^+, u_k) \quad (1)$$

and

$$\hat{P}_{k+1}^- = \tilde{F}_k P_k^+ \tilde{F}_k^T + Q_k, \quad (2)$$

where f is the dynamics model, u_k is a control vector, $F = \frac{\partial f}{\partial x}|_{x_k^+}$, and Q is our process noise which represents the uncertainty in the dynamics model. At each

time step, a measurement update is also needed. The expected measurement is computed

$$\hat{y}_{k+1}^- = h(x_{k+1}^-), \quad (3)$$

where h is the nonlinear measurement model. The measurement innovation is

$$\tilde{e}_{y_{k+1}} = y_{k+1} - \hat{y}_{k+1}^-, \quad (4)$$

where y_{k+1} is the measurement. The Kalman gain is

$$\tilde{K}_{k+1} = P_{k+1}^- \tilde{H}_{k+1}^T [\tilde{H}_{k+1} P_{k+1}^- \tilde{H}_{k+1}^T + R]^{-1}, \quad (5)$$

where $H_{k+1} = \frac{\partial h}{\partial x}|_{\hat{x}_{k+1}^-}$ and R is the measurement noise matrix. The measurement update to the state is

$$\hat{x}_{k+1}^+ = \hat{x}_{k+1}^- + \tilde{K}_{k+1} \tilde{e}_{y_{k+1}}, \quad (6)$$

and the measurement update to the covariance is

$$\hat{P}_{k+1}^+ = (I - \tilde{K}_{k+1} \tilde{H}_{k+1}) \hat{P}_{k+1}^-, \quad (7)$$

where I is the identity matrix.

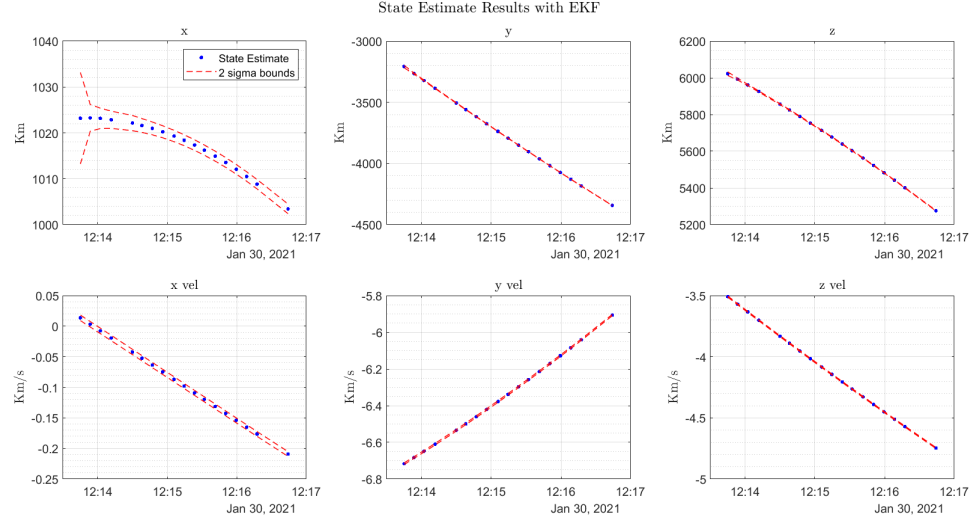


Figure 5: State estimation of satellite above Fylingdales.

Figure 5 shows the output of the EKF run on three minutes of data collected for a satellite flying over the Fylingdales radar site. For every point in time, the post measurement update is plotted for the ECI x, y, z position and velocity.

The EKF produces a covariance matrix for the states. The 2σ uncertainty bound for each of our states is the diagonal components of the covariance matrix multiplied by two. The covariance for our states gets smaller as the algorithm gets more measurements. The magnitude of the position subtracted by the Earth radius gives us the altitude which is roughly 500 km. The satellite is mostly moving in the y and z direction. The truth data for our satellites is not accurate, so we looked at the filter residuals after the measurement update, for evaluating performance. The filter residuals show where the algorithm expected the measurement versus the actual measurement.

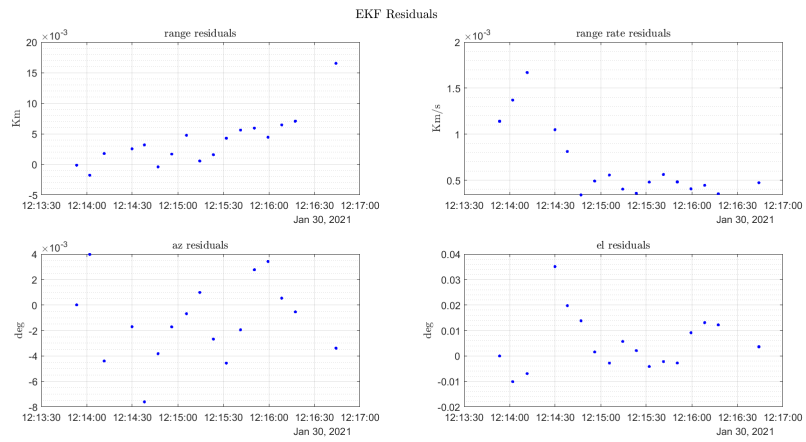


Figure 6: Filter residuals from EKF.

Figure 6 shows the filter residuals from the EKF. The magnitudes of the filter residuals are a bit higher than the measurement errors, particularly for the range and elevation. The filter residuals do not have a mean of zero for the range, and range rate. There is a clear trend in the filter residuals which could be an indication that we are not modeling the dynamics properly or there is poor state estimation. An inaccurate state propagated over long periods of time will cause data association problems in the GLMB.

2.2 Lambert's Method

Lambert's method was used to solve for the initial velocity when starting the filter. The initial position was just calculated from the first radar measurement. Lambert's method takes two ECI positions, the delta time between the positions, and uses a two-body propagator to solve for the velocity at the first radar point. Traditionally, the first two consecutive radar points in the satellite pass were used in Lambert's method to solve for the initial velocity. The filter residuals indicated that the initial velocity could be off. An experiment was done using

radar measurements further spaced a part to solve for the initial velocity to start the filter. Figure 7 shows the results of that experiment.

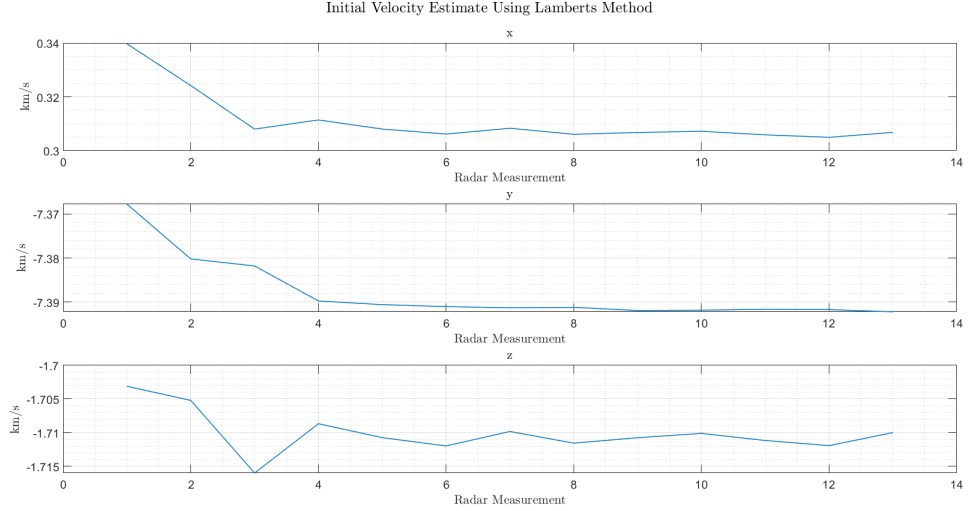


Figure 7: Initial velocity estimation using different radar points in the pass for Lambert's Method.

If there were no measurement errors and the dynamics were perfectly modeled, then the initial velocity estimate should be the same, regardless of the second radar measurement used. However, it is shown that the initial velocity estimated, when using radar points that are too close, is inconsistent with the initial velocity estimated with the second radar point further apart. As shown in the plot, the velocity estimate becomes more consistent when the radar points are further spaced. Lambert's method didn't have enough information with a short time step to get a good velocity calculation when using consecutive radar measurements. This could be due to numerical sensitivities and the algorithm not converging. The initial velocity of the satellite was calculated using the first and last radar point and the EKF was run. An experiment was done by filtering satellite measurements from Fylingdales N and propagating that state to Flyingdales SW to see how well they agree.

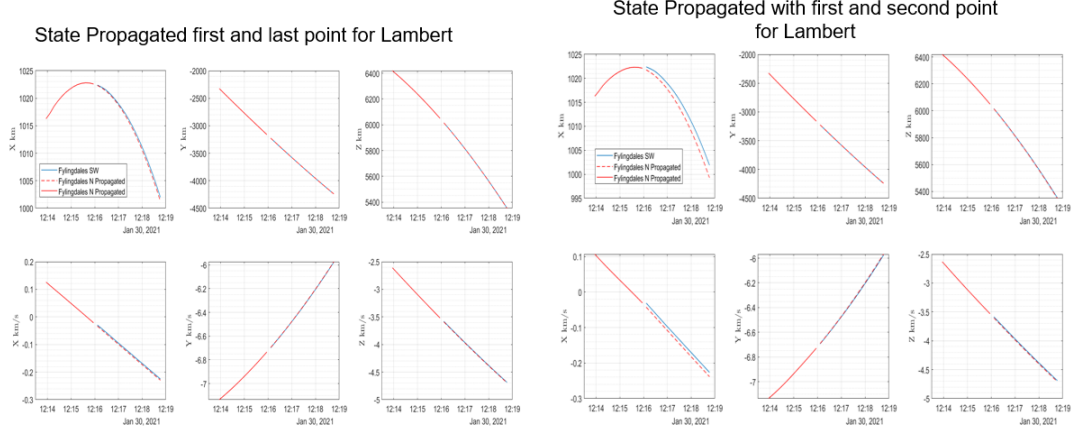


Figure 8: Comparison of starting the filter with the velocity calculated from the first two consecutive radar points versus the first and last radar point in the pass.

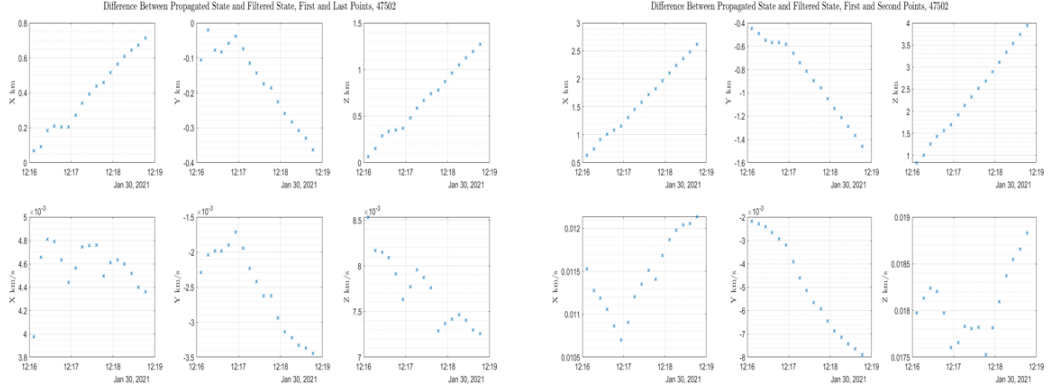


Figure 9: Difference between propagated Fylingdales N and Fylingdales SW state when starting the filter using the first two radar measurements versus the first and last measurement in the pass.

Figure 8 and Figure 9 show the results. The state from Fylingdales N, propagated to Fylingdales SW, is closer when the initial velocity is calculated using the first and last measurements as opposed to using the first two measurements in the pass. Another useful check is the filter residuals.

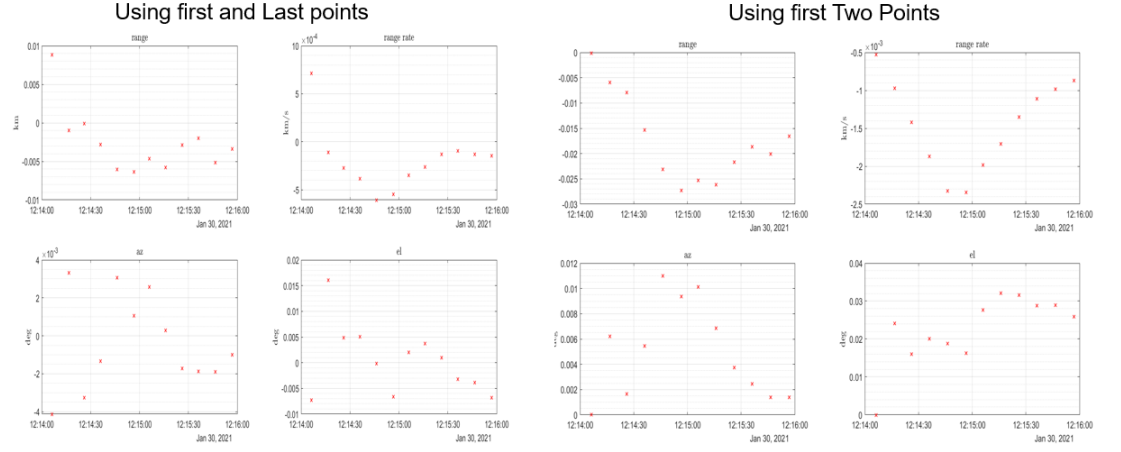


Figure 10: Filter residuals from Fylingdales N with initial velocity calculated with first two radar measurements versus initial velocity calculated from first and last radar measurements.

In Figure 10 the residuals are smaller in magnitude and closer to mean zero when the filter is initialized using the first and last measurements in the pass.

2.3 Radar Stations

These results were promising, but ideally, there would be agreement between the radar stations after long periods of propagation. The Fylingdales example was propagating the state into the next phased array, which was only about 20 seconds propagation and is still at the same radar station. A longer propagation period would be around 15 to 20 minutes. An experiment was done by propagating satellites from the Space Fence radar to the Cobra radar.

Satellite	Delta X (km)	Delta Y (km)	Delta Z (km)	Delta Vx (km/s)	Delta Vy (km/s)	Delta Vz (km/s)
47465	-14	-0.687	92.5	-1.85e-3	-103e-3	2.2e-3
47493	-13.4	-3.5	87.7	-2.5e-3	-110e-3	23e-3
47452	10.1	-57.2	-35	120e-3	-13.e-3	66e-3

Figure 11: Orbits from satellites, 47465, 47493, and 47452 in the CSPOC catalog, propagated from the Space Fence radar to the Cobra radar and differenced. This is a 16.5 minute propagation.

Figure 11 shows a 16.5 minute propagation from the Space Fence radar to the Cobra radar. Unfortunately, the orbits do not agree as there are 87

km differences in the position and 100s of m/s difference in velocity. Davies and Doctor Axelrad mentioned that the radar station's latitude, longitude, and altitude may not be correct. They found the radars on Google Earth with the associated position. After searching for the radar locations with Copilot and adjusting their position, the experiment was repeated.

Satellite	Delta X (km)	Delta Y (km)	Delta Z (km)	Delta Vx (km/s)	Delta Vy (km/s)	Delta Vz (km/s)
47465	9.8	-3.8	4.8	5.4e-3	-8.9e-3	1.2e-3
47493	2.685	1.147	-1.21	-1.35e-3	-3.7e-3	-3.35e-3
47452	2.14	7.35	-4.83	-15e-3	-13e-3	11e-3

Figure 12: Orbit from Space Fence propagated to Cobra and differenced. These results were gathered after the radar positions were adjusted.

In Figure 12 the results are much better. They are less than 10 km position error. Adjusting the radar locations could dramatically improve the GLMB results for Davies and Doctor Axelrad.

3 Conclusions

The velocity of an orbit is difficult to estimate for a satellite over a radar pass because there are few measurements. Getting accurate state estimates are important for long periods of orbit propagation without any measurements. If the propagated orbits do not agree with the measurements at the next radar, then the GLMB overestimates the number of satellites. Using radar measurements spaced out over enough time to calculate the initial velocity improves velocity estimation of an orbit.

Additionally, the radar station's location plays a huge role in the state estimation. After finding the correct radar positions, the propagated state error was reduced by over 80 km in a few examples. Finding the correct radar stations should improve the GLMB performance on real data.

References

- [1] L. Davies, P. Axelrad, (2023) *Large-Scale Satellite Deployment Tracking*
- [2] Francesco Papi, Ba-Ngu Vo, Ba-Tuong Vo, Claudio Fantacci, and Michael Beard "Generalized Labeled Multi-Bernoulli Approximation" of Multi-Object Densities", *IEEE TRANSACTIONS ON SIGNAL PROCESSING*, VOL. 63, NO. 20, OCTOBER 15, 2015
- [3] D. S. Vallado and W. D. McClain, *Fundamentals of Astrodynamics and Applications*, 4th ed. Microcosm Press, 2013.

- [4] *Space Situational Awareness.* [Online] <https://aerospace.org/ssi-space-situational-awareness>
- [5] R. H. Gooding, "A procedure for the solution of Lambert's orbital boundary-value problem," *Celestial Mechanics and Dynamical Astronomy*, col. 48, no. 2, pp. 145-165, 1990.
- [6] G. Welch, G. Bishop, *et al.*, "An introduction to the kalman filter," 1995.
- [7] J. Amos, *Spacex: World record number of satellites launched*, 2021. [Online]. Available: <https://www.bbc.com/news/science-environment-55775977>